Molecular Biology of the Cell
Vol. 17, 3651–3663, August 2006

Calsyntenin-1 Docks Vesicular Cargo to Kinesin-1[D] [V]

Anetta Konecna,*† Renato Frischknecht,*†‡ Jochen Kinter,*† Alexander Ludwig,*† Martin Steuble,*† Virginia Meskenaite,* Martin Indermühle,* Marianne Engel,* Chuan Cen,* José-Maria Mateos,§ Peter Streit,§ and Peter Sonderegger*

*Department of Biochemistry and §Brain Research Institute, University of Zurich, CH-8057 Zürich, Switzerland; and ‡Leibniz Institute for Neurobiology, 39 118 Magdeburg, Germany

Submitted February 7, 2006; Revised May 8, 2006; Accepted May 31, 2006
Monitoring Editor: Randy Schekman

We identified a direct interaction between the neuronal transmembrane protein calsyntenin-1 and the light chain of Kinesin-1 (KLC1). GST pulldowns demonstrated that two highly conserved segments in the cytoplasmic domain of calsyntenin-1 mediate binding to the tetratricopeptide repeats of KLC1. A complex containing calsyntenin-1 and the Kinesin-1 motor was isolated from developing mouse brain and immunoelectron microscopy located calsyntenin-1 in association with tubulovesicular organelles in axonal fiber tracts. In primary neuronal cultures, calsyntenin-1–containing organelles were aligned along microtubules and partially colocalized with Kinesin-1. Using live imaging, we showed that these organelles are transported along axons with a velocity and processivity typical for fast axonal transport. Point mutations in the two kinesin-binding segments of calsyntenin-1 significantly reduced binding to KLC1 in vitro, and vesicles bearing mutated calsyntenin-1 exhibited a markedly altered anterograde axonal transport. In summary, our results indicate that calsyntenin-1 links a certain type of vesicular and tubulovesicular organelles to the Kinesin-1 motor.

INTRODUCTION

The development of a dendritic arborization and the extension of axons are key features of neuronal maturation (Bradke and Dotti, 2000; Jan and Jan, 2001; Scott and Luo, 2001). Both processes involve surface expansion of the plasma membrane, which requires an abundant production of lipids and proteins and their efficient delivery from the cell body to the growing tips of dendrites and axons (Vogt *et al.*, 1996; Bradke and Dotti, 2000; Martinez-Arca *et al.*, 2001). Fast anterograde axonal transport is mediated by kinesins, molecular motors that transport their cargos along microtubules toward the plus end. The first kinesin motor, Kinesin-1, was identified as a motor protein for vesicle and organelle movement in both squid and vertebrate axons (Brady, 1985; Vale *et al.*, 1985; Hirokawa, 1998). Kinesin-1 is composed of two kinesin heavy chains (KHC) and two kinesin light chains (KLC; Hirokawa *et al.*, 1989). In the mouse, both the KHCs (KIF5A, KIF5B, and KIF5C) and the KLCs (KLC1, KLC2) are encoded by different genes with distinct expression patterns (Rahman *et al.*, 1998; Xia *et al.*, 1998). KIF5A, KIF5C, and KLC1 are enriched in neural tissues, whereas KIF5B and KLC2 are ubiquitously expressed. The N-terminal globular head domain of KHC is responsible for the force-generating motor activity and for binding to microtubules. The site of interaction with the cargo has been attributed to the C-terminal tail domain of KHCs (Setou *et al.*, 2002) and/or to the TPR (tetratricopeptide repeat) domains of KLCs (Verhey *et al.*, 1998; Bowman *et al.*, 2000). TPRs are loosely conserved, 34-amino acid long sequence motives that are arranged in tandem repeats. They mediate protein–protein interactions and assembly of multiprotein complexes and are found in a number of functionally different proteins (Blatch and Lassle, 1999). TPR modules are particularly versatile antiparallel α-helical structures arranged to form an amphipathic groove suitable for the specific recognition of and binding to relatively short, linear peptides (Terlecky *et al.*, 1995; Scheufler *et al.*, 2000).

Kinesin-1 motors mediate the transport of various membranous organelles (Hirokawa and Takemura, 2005), but the mechanism how they recognize and bind to a specific cargo has not yet been completely elucidated. Several motor protein receptors and adaptors have been identified, including the integral membrane proteins ApoER2 (Stockinger *et al.*, 2000), the β-amyloid precursor protein (APP; Kamal *et al.*, 2000, 2001) and the membrane-associated proteins of the c-Jun N-terminal kinase (JNK)-interacting protein (JIP) family (Bowman *et al.*, 2000; Verhey *et al.*, 2001). JIP-1 and JIP-2 dock Kinesin-1 to vesicles via interaction with the reelin receptor ApoER2 (Stockinger *et al.*, 2000). JIP-3/SYD/Unc16 is structurally unrelated to JIP-1/-2 and links Kinesin-1 to an unidentified cargo. APP was shown to interact directly with the Kinesin-1 motor (Kamal *et al.*, 2000, 2001), yet recent evidence indicates that the attachment of APP to Kinesin-1 is not direct (Lazarov *et al.*, 2005) but may require JIP-1/JIP-2 (Inomata *et al.*, 2003; Matsuda *et al.*, 2003).

Calsyntenins are type-1 neuronal transmembrane proteins of the cadherin superfamily and, in the adult brain, found in the postsynaptic membrane (Vogt *et al.*, 2001). In humans

This article was published online ahead of print in *MBC in Press* (http://www.molbiolcell.org/cgi/doi/10.1091/mbc.E06–02–0112) on June 7, 2006.

[D] [V] The online version of this article contains supplemental material at *MBC Online* (http://www.molbiolcell.org).

† These authors contributed equally to this work.

Address correspondence to: Peter Sonderegger (pson@bioc.unizh.ch).

Abbreviations used: KHC, kinesin heavy chain; KLC, kinesin light chain; TPR, tetratricopeptide repeat; Cst, calsyntenin; KBS, KLC1-binding segment; wt, wild-type; W1, calsyntenin-1 mutated in KBS1; W2, calsyntenin-1 mutated in KBS2; WW, calsyntenin-1 mutated in KBS1 and KBS2; DIV, day in vitro; aa, amino acid.

and mice, three calsyntenin genes have been identified (Hintsch *et al.*, 2002). Calsyntenin-1 was originally identified as a protein transported along neurites and released from embryonic chicken motoneurons by proteolytic cleavage. Although the released ectodomain accumulates in the cerebrospinal fluid, the transmembrane stump is internalized into the synaptic spine apparatus (Vogt *et al.*, 2001). Recently, it was suggested that calsyntenins (also termed alcadeins) and APP undergo similar and coordinated proteolytic processing, which may be regulated by X11L/Mint2 (Araki *et al.*, 2003).

Prompted by a yeast two-hybrid screen, we found and characterized a direct interaction between the cytoplasmic domain of calsyntenin-1 and KLC1. The binding of calsyntenin-1 to the TPR domains of KLC1 is mediated by two conserved motives. In growth cones of primary cortical neurons, we found calsyntenin-1 in a subset of vesicles that are aligned along microtubules and have dynamic properties typical for kinesin-mediated transport. We finally show that vesicles containing mutated calsyntenin-1 with reduced KLC1-binding affinity display a markedly altered transport behavior. Thus, calsyntenin-1 represents a novel cargo-docking protein for Kinesin-1–mediated vesicular transport.

MATERIALS AND METHODS

Yeast Two-Hybrid Screen

As bait we used a C-terminal fragment (amino acids 878-924) of murine calsyntenin-1 (accession NP_075538.1) in-frame with the lexA DNA-binding domain that was subcloned into the DUALhybrid bait vector (Dualsystems, Zurich, Switzerland). Yeast cells expressing the bait were transformed with plasmids from an embryonic mouse brain cDNA library (Clontech BD Biosciences, Palo Alto, CA). Positive clones were isolated and characterized by sequencing.

Antibodies

Polyclonal rabbit antibodies R85, R113, and R140 were generated against murine calsyntenin-1. R85 antibodies were raised against a recombinant protein corresponding to residues 43-295. R113 antibodies were raised against a mixture of four peptides: METYEDQHSSEEE, DGEEEEDITSAESESSE, EGGPGDGQNATRQLEWDD, and DGQNATRQLEWDDSTLSY. Polyclonal antibody R140 was raised against the latter two peptides, which span the very C-terminus. All antibodies were affinity-purified and used at a concentration of 0.5–1 μg/ml. Antibodies R85 and R140 were tested by Western blotting and immunocytochemistry (Supplementary Figure 1). Monoclonal antibodies against synaptophysin (MAB5258), KHC H2 (MAB1614), GAP-43 (MAB347), Tau-1 (MAB3420), GFAP (MAB360), and MAP2 (MAB3418) were from Chemicon (Temecula, CA). The monoclonal antibody (mAb) against tubulin (DM1A) was from Sigma (St. Louis, MO). Polyclonal antibodies to KLC (L15), rabbit anti-HA (Y-11) and rabbit anti-c-myc (A-14) were from Santa Cruz Biotechnology (Santa Cruz, CA). Monoclonal mouse anti-GFP and mouse anti-HA (12CA5) were from Roche (Indianapolis, IN). Monoclonal anti-JIP-1 and anti-SNAP-25 antibodies were from Transduction Laboratories (Lexington, KY). The anti-KLC antibody KLC63–90 was a kind gift of Scott T. Brady (University of Illinois, Chicago). Fluorescent secondary antibodies (Cy3- and FITC-conjugated) were from Jackson ImmunoResearch Laboratories (West Grove, PA) and used at 2.5 μg/ml. Horseradish peroxidase (HRP)-conjugated secondary antibodies were from Kirkegaard & Perry Laboratories (Gaithersburg, MD), Bio-Science Products (Rockville, MD) and Chemicon.

Recombinant Proteins

Glutathione-*S*-transferase (GST) fusion proteins of cytoplasmic segments of the murine calsyntenins were produced by PCR amplification of the corresponding cDNA segments and ligation into the pGEX-6P-1 vector (Amersham, Piscataway, NJ). The following GST fusion proteins were constructed: Cst1 (aa 878-979; accession number NP_075538.1), Cst2 (aa 858-966; NP_071714.2), Cst3 (aa 869-956; NP_705728.1), Cst1/911ΔC (aa 878-911), Cst1/906ΔC (aa 878-906), Cst1/902ΔC (aa 878-902), Cst1/897-911 (aa 897-911), Cst1/903-911 (aa 903-911), and Cst1/966-979 (aa 966-979). GST-Cst1-W903/A (W1 mutant), GST-Cst1-W972/A (W2 mutant), and GST-Cst1-WW/AA (WW mutant) were generated from GST-Cst1 by PCR. To generate EGFP-Cst1 mutants, the cytoplasmic segment of EGFP-Cst1 was replaced with the mutant sequences. Mutants E900/A, M901/A, D902/A, D904/A, and D905/A were cloned into the GST-Cst1/897-911 background. GST-Cst3Δ bears the Cst3 cytoplasmic segment from amino acids 891-956 and GST-Cst3Δ-F896/D is the corresponding mutant. All constructs were verified by sequencing. Proteins were expressed in *Escherichia coli* strain BL21 under standard conditions and purified with glutathione-Sepharose 4B (Amersham).

Murine kinesin light chain 1 was amplified from cDNA by PCR and cloned into pGEX-6P-1. HA-KLC1 was generated by fusion of the hemagglutinin tag (YPYDVPDYA) in frame with the cDNA for KLC1 into pcDNA3.1. EGFP-calsyntenin-1 was cloned by insertion of the EGFP cDNA (Invitrogen, Carlsbad, CA) in-frame with the cDNA for wild-type (wt) or mutant forms of calsyntenin-1 into pcDNA3.1. The KLC1 construct HA-L176 and myc-KHC were kindly provided by Bruce J. Schnapp (Oregon Health & Science University) and have been described previously (Verhey *et al.*, 1998).

GST Pulldown Assay

GST pulldown assays were performed as described previously (Kamal *et al.*, 2000) with minor modifications. Purified GST, GST-Cst1, GST-Cst2, and GST-Cst3 (5 μg) bound to glutathione-Sepharose 4B beads were incubated with 15 μg of purified KLC1 in 200 μl buffer A (50 mM KCl, 100 mM NaCl, 2 mM $CaCl_2$, 2 mM $MgCl_2$, 5 mM DTT, 20 mM Tris-Cl, pH 7.5), containing 1% ovalbumin, and protease inhibitors for 1 h at 4°C. After washing the beads five times with buffer A, bound proteins were eluted with SDS-PAGE loading buffer and analyzed by Western blotting.

To estimate the apparent binding affinity of calsyntenin-1 to KLC1, 46 nM GST-Cst1 immobilized on beads was incubated with increasing concentrations (0.2–5 μM) of recombinant KLC1. Bound proteins and known amounts of KLC1 were resolved on 4–12% NuPAGE gels (Invitrogen), stained with the fluorescent dye SYPRO Ruby (Molecular Probes, Eugene, OR) and scanned using Typhoon 9400 (Molecular Dynamics, Sunnyvale, CA). The amounts of bound KLC1 and coupled GST-Cst1 were determined from fluorescence measurements using ImageQuant 5.0 (Molecular Dynamics) software. The molar ratio of bound KLC1 over bound GST-Cst1 at each point was calculated and plotted against the concentration of free KLC1. The concentration of free KLC1 was deduced by subtracting the amount of bound KLC1 from total KLC1 in the reaction. The apparent dissociation constant K_d was obtained by nonlinear regression fitting of the binding curve to the equation $Y = B_{max} * X/(K_d + X)$ using Prism v.4 (GraphPad software, San Diego, CA), where Y is the concentration of bound KLC1 and X is the concentration of free KLC1, B_{max} is the maximal binding and K_d is the concentration of ligand (KLC1) required to reach half-maximal binding. For quantitative GST pulldowns of calsyntenin-1 tryptophan mutants, equal amounts of GST, wt, or mutant GST-Cst1 (2 μg) were incubated with KLC1 (25 μg). The apparent binding affinities of the mutant proteins were expressed as percent bound KLC1 relative to wt calsyntenin-1. Statistical analyses were performed using the two-tailed *t* test.

HeLa Cell Culture and Immunoprecipitation

HeLa cells were grown in DMEM supplemented with 5 mM glutamine, 1 mM sodium pyruvate, and 10% fetal calf serum (FCS). Transfections were performed with Fugene6 according to the manufacturer's recommendations (Roche). Twenty-four hours after transfection, cells were lysed in NP-40 buffer (1% NP-40, 150 mM NaCl, 5 mM EDTA, 1 mM Na_3VO_4, 5 mM NaF, 50 mM Tris-HCl, pH 8), supplemented with protease inhibitor cocktail (Roche). Cell lysate (100–200 μg) was incubated with 2–4 μg affinity-purified IgG for 2 h at 4°C. Antibody-antigen complexes were recovered with 10 μl protein A-Sepharose preblocked with 5% ovalbumin in NP-40 buffer for 1 h at 4°C. Beads were washed four times with NP-40 buffer and then boiled in SDS-PAGE loading buffer.

Subcellular Fractionation and Immunoprecipitation from Mouse Brain

The V1 membrane fraction was prepared by differential centrifugation as described previously (Morfini *et al.*, 2001a, 2001b). Growth cone particles (GCP), growth cone vesicles (GCV), and growth cone membranes (GCM) were prepared from P7 mouse forebrains as described previously (Pfenninger *et al.*, 1983; Igarashi *et al.*, 1997). For further details see Supplementary Material.

For immunoprecipitation from V1 fractions, membrane pellets were solubilized for 30 min at 4°C in IP buffer (75 mM NaCl, 5 mM EDTA, 5 mM *N*-ethylmaleimide, 10 mM CHAPS, 50 mM Tris-HCl, pH 7.5) supplemented with protease inhibitor cocktail (Roche) and cleared by ultracentrifugation. Membrane extracts were precleared on protein A-Sepharose beads for 1 h at 4°C and then incubated with 6 μg of affinity-purified antibody R85 or unrelated rabbit IgG for 2 h at 4°C, before adding 10 μl protein A-Sepharose for an additional 1 h at 4°C. The immunoprecipitates were washed five times with IP buffer and twice with 50 mM Tris-HCl buffer, pH 7.5, containing 130 mM NaCl. Equivalent amounts of immunoprecipitates were loaded on 4–12% NuPAGE gels (Invitrogen) and subjected to Western blotting.

Neuronal Cultures

Primary dissociated cortical and hippocampal cultures were prepared from embryonic day 18 Sprague Dawley rats. Cell suspensions were plated onto poly-L-lysine–coated (Sigma) glass coverslips and transferred onto a monolayer of astrocytes (Banker, 1980). Cells were grown in DMEM supplemented

with B27, 5 mM glutamine, 1 mM sodium pyruvate, and 0.5 mg/ml Albumax. All chemicals used for neuronal cultures were obtained from Invitrogen, unless indicated otherwise.

For immunofluorescence analysis cells were fixed either in 4% paraformaldehyde (PFA), 4% sucrose in phosphate-buffered saline (PBS), pH 7.4, for 10 min at 37°C or in methanol for 10 min at −20°C. Samples were blocked for 1 h in 10% FCS, 0.1% glycine, and 0.2% saponin in PBS. Cells were then stained with primary and secondary antibodies in 0.1% saponin in PBS o/n and for 1 h at 4°C, respectively. Images were taken with a Leica confocal microscope TCS-SP1 (Deerfield, NY) unless otherwise stated.

Live Imaging Microscopy

For live imaging, cortical neurons were transfected on 3 days in vitro (DIV) with expression vectors for the respective EGFP-fusion proteins using Lipofectamine 2000 (Invitrogen). Live imaging was performed 24–36 h after transfection at 37°C using an inverted microscope (Eclipse TE300, Nikon, Melville, NY) equipped with a Plexiglas box to maintain a stable atmosphere (Life Imaging Services, Reinach, Switzerland). Images were collected with a SensiCAM QE camera (Cooke, Auburn Hills, MI) controlled by Metamorph Imaging software (Universal Imaging, West Chester, PA), using a 100× objective (N.A. 1.4), a standard FITC filter set, and a Lambda DG-4 light source (Sutter Instrument, Novato, CA). Images were captured every 2 s for a period of 2–3 min under constant perfusion with 119 mM NaCl, 2.5 mM KCl, 2 mM $CaCl_2$, 2 mM $MgCl_2$, 30 mM glucose, and 25 mM HEPES, pH 7.4. Axons were selected based on their unique length, which exceeded dendritic processes at least fivefold. Speed and the run-lengths of organelles were determined by measuring the distance covered between two successive frames using the manual tracking function of ImageJ (National Institutes of Health). All data were exported to Excel and statistically analyzed using the two-tailed *t* test.

RESULTS

Calsyntenin-1 Interacts with Kinesin Light Chain 1 through Two Conserved Binding Segments

To identify proteins that interact with the cytoplasmic domain of calsyntenin-1, we performed a yeast two-hybrid screen. A bait construct encoding a fusion protein containing the proximal part of the cytoplasmic region (aa 878-924) of murine calsyntenin-1 (Figure 1A) was used to screen a fetal murine brain cDNA library. The acidic stretch in the cytoplasmic segment was excluded from the bait because its presence had resulted in self-activation. In a screen of 10^6 independent transformants, 17 positive clones were isolated. Sequence analysis revealed that 16 clones contained KLC1 and one KLC2 (Figure 1B). In 14 of the 16 KLC1-containing clones, the full KLC1 sequence was found. One clone lacked the N-terminal heptad repeat and one clone contained only the C-terminal TPR domains.

Next, we investigated the KLC1 binding of all three calsyntenins by in vitro GST pulldown assays. Equal amounts of GST fusion proteins were immobilized on glutathione-Sepharose beads and incubated with bacterially expressed KLC1. GST-calsyntenin-1 and -2 pulled down similar amounts of KLC1, whereas GST-calsyntenin-3 was less efficient (Figure 1C). No binding of KLC1 to GST was observed. To estimate the strength of the interaction between the cytoplasmic segment of calsyntenin-1 and KLC1, 46 nM GST-calsyntenin-1 were incubated with KLC1 concentrations ranging from 0.2 to 5 μM. Bound and free KLC1 as well as GST-calsyntenin-1 were quantified. The apparent dissociation constant between KLC1 and the complete cytoplasmic segment of calsyntenin-1 was determined to be 1.7 ± 0.25 μM (Figure 1D). In addition, these binding studies revealed that saturation of GST-calsyntenin-1 was reached when 0.5 KLC1 molecules were bound. This indicates that one KLC1 molecule may bind two cytoplasmic segments of calsyntenin-1.

Bacterially expressed KLC1, in particular the TPR domains, have recently been shown to exhibit considerable nonspecific binding properties, possibly due to misfolding in *E. coli* (Lazarov *et al.*, 2005). Therefore, we tested the interaction of calsyntenin-1 with native and recombinant KLC1 expressed in HeLa cells. In GST pulldown assays using mouse brain extract, GST-calsyntenin-1 pulled down both light and heavy chain of Kinesin-1 (Figure 1E). We then performed coimmunoprecipitations from protein extracts of HeLa cells cotransfected with N-terminally EGFP-tagged calsyntenin-1 and HA-tagged wt KLC1. Polyclonal antibodies directed against the N-terminus of calsyntenin-1 (R85) coimmunoprecipitated HA-KLC1, whereas anti-HA antibodies coimmunoprecipitated EGFP-calsyntenin-1 (Figure 1F1). Both proteins were also specifically coimmunoprecipitated with anti-GFP antibodies and R140, an antibody directed against the C-terminus of calsyntenin-1, but not with R140 preimmune IgG. In addition, R140, R85, and anti-GFP antibodies did not immunoprecipitate HA-KLC1 from extracts of mock-transfected HeLa cells (Supplementary Figure 2). Finally and consistent with our yeast two-hybrid screen, a KLC1 construct lacking all TPR domains (construct HA-L176; Verhey *et al.*, 1998) did not coimmunoprecipitate with calsyntenin-1 (Figure 1F2). Altogether, these results indicate that the interaction between calsyntenin-1 and KLC1 is specific and requires the TPR repeats of KLC1.

To localize the KLC1-binding site within the cytoplasmic domain of calsyntenin-1, several deletion mutants were constructed from the C-terminus of the bait construct and tested for interaction with KLC1 in an in vitro GST pulldown assay (Figure 2, A and B). Constructs 911ΔC and 906ΔC were still able to bind KLC1, whereas binding was abolished after removal of four additional amino acids (902ΔC). Therefore, we assumed that the amino acid sequence -Trp-Asp-Asp-Ser- (WDDS) was important for KLC1 binding. Further deletions N-terminally of the WDDS motif revealed a minimal KLC1-binding site (aa 897-906), which we termed KLC1-binding segment 1 (KBS1). As shown in Figure 2C, the WDDS motif is preserved in all members of the calsyntenin family. Because calsyntenin-1 contains a second WDDS motif close to the C-terminus, a GST fusion protein comprising the last 14 amino acids of calsyntenin-1 (aa 966-979) was tested for binding to KLC1. This segment was able to interact with KLC1 as well (Figure 2A) and was thus termed KLC1-binding segment 2 (KBS2). We concluded that the cytoplasmic domain of calsyntenin-1 contains two KLC1-binding segments: KBS1 and KBS2.

We introduced single point mutations into the KLC1-binding segments KBS1 and KBS2 and analyzed their effect by GST pulldowns (Figure 2, D and E). We found that replacement of the tryptophans (W903/A, W972/A) by alanine in either of the kinesin-binding segments (mutants W1 and W2) reduced binding to KLC1 to ~30% compared with wt calsyntenin-1. When the tryptophans of both kinesin-binding segments were mutated to alanine (mutant WW), only ~3% of the wt binding was measured. We also tested the effect of these mutations in coimmunoprecipitations from HeLa cells cotransfected with full-length EGFP-calsyntenin-1 or the corresponding mutant constructs and HA-KLC1 (Figure 2F). In accordance with the in vitro binding assays, a markedly reduced KLC1 binding of the double-mutant (WW) was observed. However, the single-mutants (W1, W2) precipitated amounts of HA-KLC1 similar to that of wt calsyntenin-1. These results indicate that one functional KLC1-binding site of calsyntenin-1 is sufficient to mediate the interaction and that mutation of both binding sites impairs but does not abolish binding to KLC1 in live cells.

We next analyzed the contribution of each amino acid in the KBS1 core motif on KLC1 binding in GST pulldowns. Replacement of residues E900 and D902 with alanine markedly reduced the amount of bound KLC1. The D904/A and

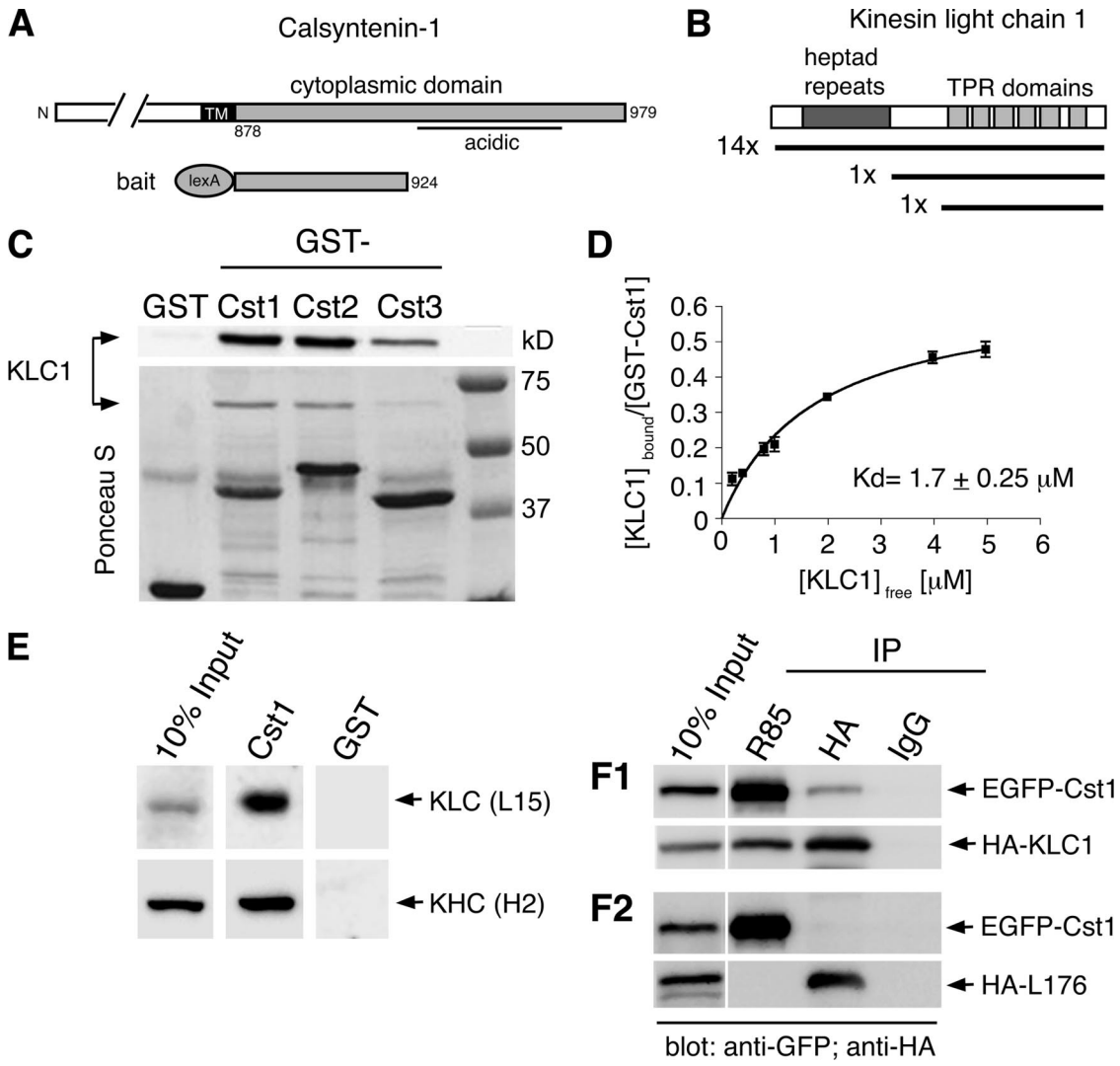

Figure 1. The cytoplasmic segment of calsyntenin-1 binds directly to the light chain of Kinesin-1. (A) Schematic diagram illustrating the calsyntenin-1 bait construct (aa 878-924) used for the yeast two-hybrid screen. (B) Domain structure of KLC1. The regions encoding the 16 KLC1 cDNA clones isolated from the screen are depicted. (C) Recombinant KLC1 (15 μg) was incubated with beads coated with 5 μg GST or GST-calsyntenin fusion proteins (GST-Cst1, GST-Cst2, GST-Cst3). Bound proteins were analyzed by immunoblotting using an antibody against KLC1 (L15; top panel) and Ponceau-S staining of the membrane (bottom panel). All three calsyntenins interact with KLC1. (D) Estimation of the apparent binding affinity of calsyntenin-1 to KLC1. Increasing concentrations of KLC1 (0.2–5 μM) were incubated with 46 nM GST-Cst1. Bound and free KLC1 were measured, and the K_d was determined by curve-fitting as described in *Materials and Methods* (R^2 = 0.95, n = 3). (E) Immobilized GST-Cst1 or GST (50 μg) was incubated with mouse brain extract. Bound proteins were analyzed by immunoblotting using the indicated antibodies. GST-Cst1 pulled down both KLC1 and KHC. (F1 and F2) HeLa cells were cotransfected with EGFP-calsyntenin-1 and HA-KLC1 (F1) or the KLC1 deletion construct HA-L176 (F2) followed by immunoprecipitations using the indicated antibodies. Immunoprecipitates were analyzed by immunoblotting with the indicated antibodies. EGFP-calsyntenin-1 coimmunoprecipitated with HA-KLC1, but not with HA-L176.

D905/A mutations, as well as the M901/A mutation, almost completely abolished binding to KLC1 (Figure 2G). Furthermore, replacement of F896 with aspartate (F896/D) in the calsyntenin-3 KBS increased binding to KLC1 (Figure 2H), suggesting that F896 is responsible for the lower apparent binding affinity of calsyntenin-3 when compared with calsyntenin-1 and -2 (Figure 1C). In conclusion, we showed that the two kinesin-binding segments KBS1 and KBS2 mediate binding to KLC1 in vitro and in cotransfected HeLa cells and that the conserved tryptophan residues as well as the surrounding amino acids are relevant for the interaction.

Calsyntenin-1 Interacts with Kinesin-1 In Vivo

To address the question whether calsyntenin-1 interacts with the complete Kinesin-1 complex in live cells, we carried out coimmunoprecipitations from HeLa cells that were triple-transfected with full-length EGFP-calsyntenin-1, HA-KLC1, and myc-KHC (Figure 3A). Antibodies against HA- and myc-tags efficiently precipitated the Kinesin-1 heterotetramer together with a considerable amount of calsyntenin-1. Likewise, antibody R85 directed against calsyntenin-1 coimmunoprecipitated both HA-KLC1 and myc-KHC, whereas nonimmune IgG did not precipitate any of these proteins.

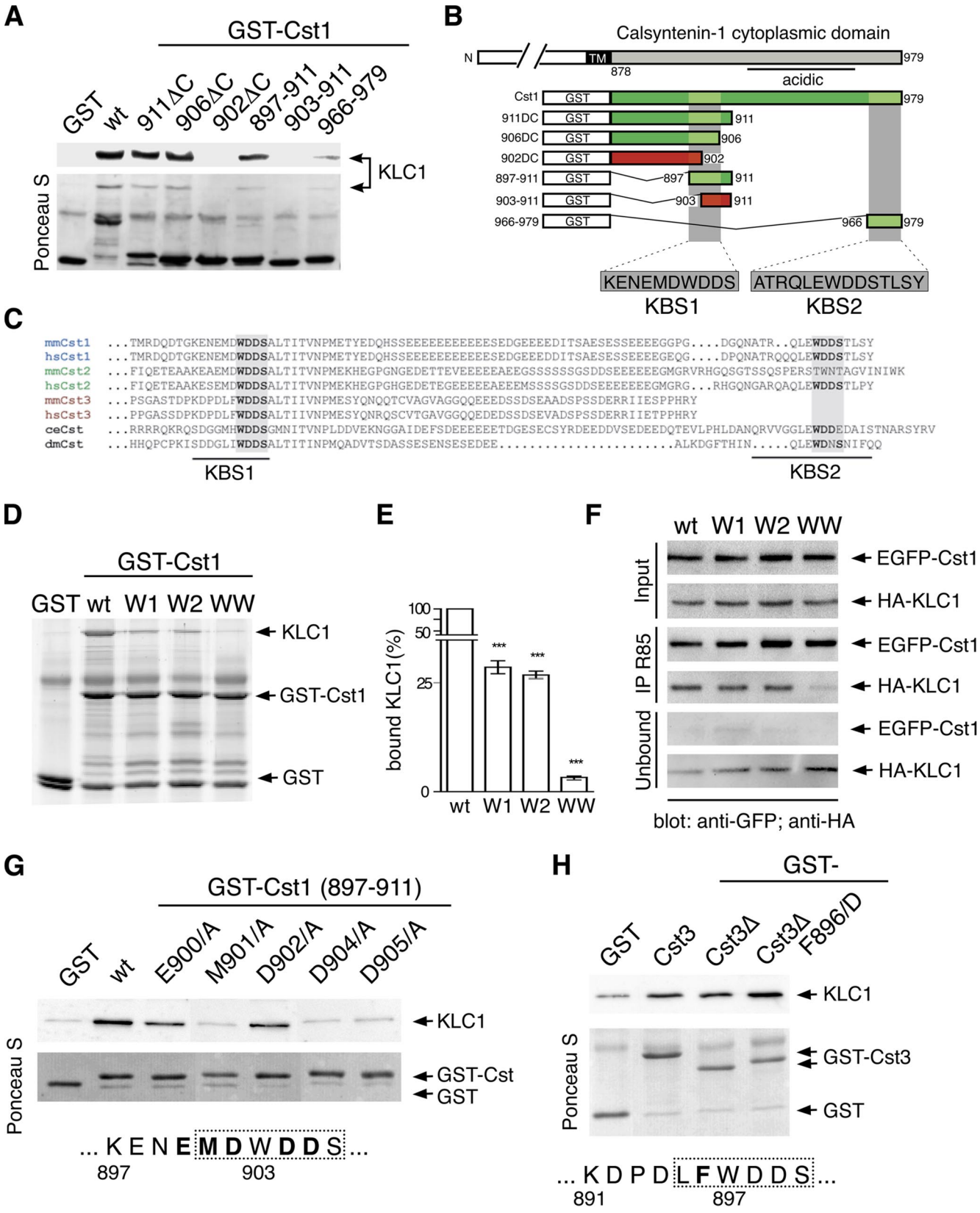

Figure 2. Calsyntenin-1 contains two KLC1-binding segments. (A) Deletion mutants of the cytoplasmic domain of calsyntenin-1 were tested for KLC1 binding in GST pulldown assays as described in Figure 1C. Two KLC1-binding segments, KBS1 (aa 897-906) and KBS2 (aa 966-979), were found. (B) Schematic diagram summarizing the mapping analysis. Binding constructs are shown in green and nonbinding mutants in red. (C) Sequence alignment of the cytoplasmic domain of calsyntenins. Note the conservation of the WDDS core motif in KBS1 and KBS2. (D) Calsyntenin-1 point mutants in the KBS1 and KBS2 were generated by replacing the conserved tryptophan residues with alanine in either

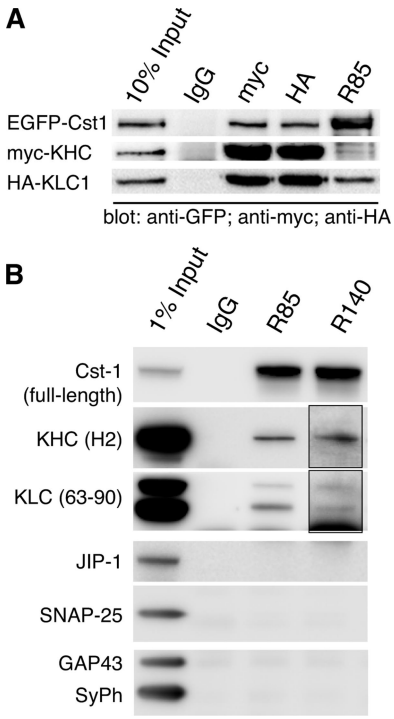

Figure 3. Calsyntenin-1 and Kinesin-1 interact in live cells. (A) HeLa cells were triple-transfected with EGFP-calsyntenin-1, HA-KLC1, and myc-KHC. Cell lysates were subjected to immunoprecipitation using the indicated antibodies. The tripartite complex was isolated with R85, anti-HA, and anti-c-myc antibodies, but not with nonspecific IgG. (B) Immunoprecipitation of calsyntenin-1 from the V1 membrane fraction of P7 mouse brains (see Supplementary Methods). Antibody R85 and R140 immunoprecipitates contained KLC1, KLC2, and KHC, but not JIP-1, SNAP-25, synaptophysin, and GAP-43. Nonspecific IgG did not precipitate any of these proteins. Note that longer exposure times were required to detect KLC and KHC in R140 immunoprecipitates (insets).

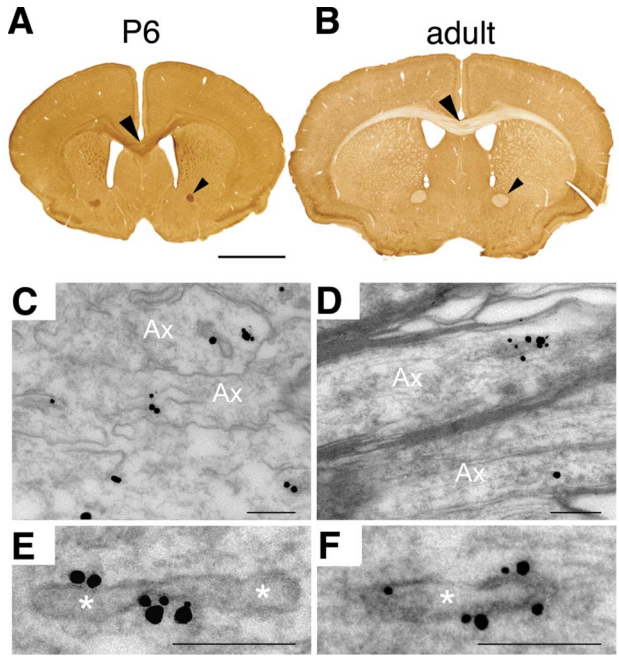

Figure 4. Calsyntenin-1 is enriched in developing nerve fiber tracts and is associated with tubulovesicular organelles. (A and B) Immunohistochemistry of P6 and adult mouse brain using anti-calsyntenin-1 antibody R113. (A) At P6 all major fiber tracts were strongly labeled, including the anterior commissure (small arrowhead) and the corpus callosum (large arrowhead). (B) In adult mice, only faint immunoreactivity was observed in these tracts. (C–F) Immunoelectron micrograph of calsyntenin-1 in the corpus callosum of P8 mice using antibody R113. Immunogold particles labeled the membranes of tubulovesicular organelles. Scale bar, 2 mm in A and B, 0.2 μm in C–F.

To investigate the calsyntenin-1/Kinesin-1 interaction in mouse brain, we first analyzed the temporal expression pattern of the two proteins by Western blotting of mouse brain homogenates from different developmental stages. Both calsyntenin-1 and Kinesin-1 expression gradually increased during the first postnatal week, reaching a peak at postnatal day (P) 7 (Supplementary Figure 3A). We then examined the distribution of both proteins in P7 mouse brains by differential centrifugation. To minimize the release of Kinesin-1 from membrane-bounded organelles during fractionation, we used a combination of EDTA and *N*-ethylmaleimide as described previously (Tsai *et al.*, 2000; Morfini *et al.*, 2001a). The bulk of KHC and KLC was found associated with the three membrane fractions (V0, V1, and V2). The full-length form of calsyntenin-1 was particularly enriched in the V1 fraction, whereas the transmembrane stump was found in both V0 and V1 (Supplementary Figure 3B). Because full-length calsyntenin-1 and Kinesin-1 cofractionated in V1 of P7 brains, we performed coimmunoprecipitations from these membranes under the conditions described above (Figure 3B). Using antibody R85, we immunoisolated complexes containing calsyntenin-1, KLC1, KLC2, and KHC. Antibody R140 also coimmunoprecipitated the Kinesin-1 motor, but was less efficient than R85, most likely because the peptide antigens used to generate the R140 span the KBS2 of calsyntenin-1. Unrelated IgG precipitated neither KLC nor KHC. In addition, two other Kinesin-1 ligands, JIP-1 (Verhey *et al.*, 2001) and SNAP-25 (Diefenbach *et al.*, 2002), as well as GAP43 and synaptophysin, both highly abundant in V1 membranes, were not present in R85 or R140 immunoprecipitates. These results indicate that calsyntenin-1 and the Kinesin-1 motor form a complex in vivo.

Calsyntenin-1 Is Associated with Axonal Tubulovesicular Organelles In Vivo

To assess the spatial distribution of calsyntenin-1 in mouse brain, we performed immunohistochemistry using an affin-

Figure 2 (cont). of the two binding sites (W1 and W2) or in both (WW) and tested in GST pulldowns as described in Figure 1C. (E) Analysis of KLC1-binding of calsyntenin-1 point mutants by quantitative GST pulldown assay. The apparent binding affinities of W mutant proteins are expressed as amount of bound KLC1 relative to the amount bound by wild-type GST-Cst1. Mutation in one binding segment (W1 and W2) caused a significant reduction of bound KLC1 to <30%. Mutation of both tryptophans (WW) reduced KLC1-binding to 3% (***$p < 0.0001$; $n = 3$). (F) HeLa cells were cotransfected with wild-type or mutant EGFP-calsyntenin-1 constructs and HA-KLC1 followed by immunoprecipitation using antibody R85. Note the reduction of bound HA-KLC1 and the relative abundance of unbound HA-KLC1 in WW mutant precipitates. (G) Effect of several KBS1 point mutations on KLC1-binding. Immobilized GST-Cst1 (897-911) and the corresponding point mutants were incubated with KLC1. Bound proteins were analyzed by immunoblotting. The MDWDDS core motif of KBS1 is boxed, and the mutated amino acid residues are depicted in bold. (H) Effect of phenylalanine F896 in the KBS of calsyntenin-3 on KLC1 binding. Immobilized GST-calsyntenin-3 (aa 869-956), GST-Δcalsyntenin-3 (891-956), and the corresponding F896/D mutant were incubated with KLC1. Bound proteins were analyzed by immunoblotting. mm, *Mus musculus*; hs, human; dm, *D. melanogaster*; ce, *C. elegans*. Error bars in E, SEM.

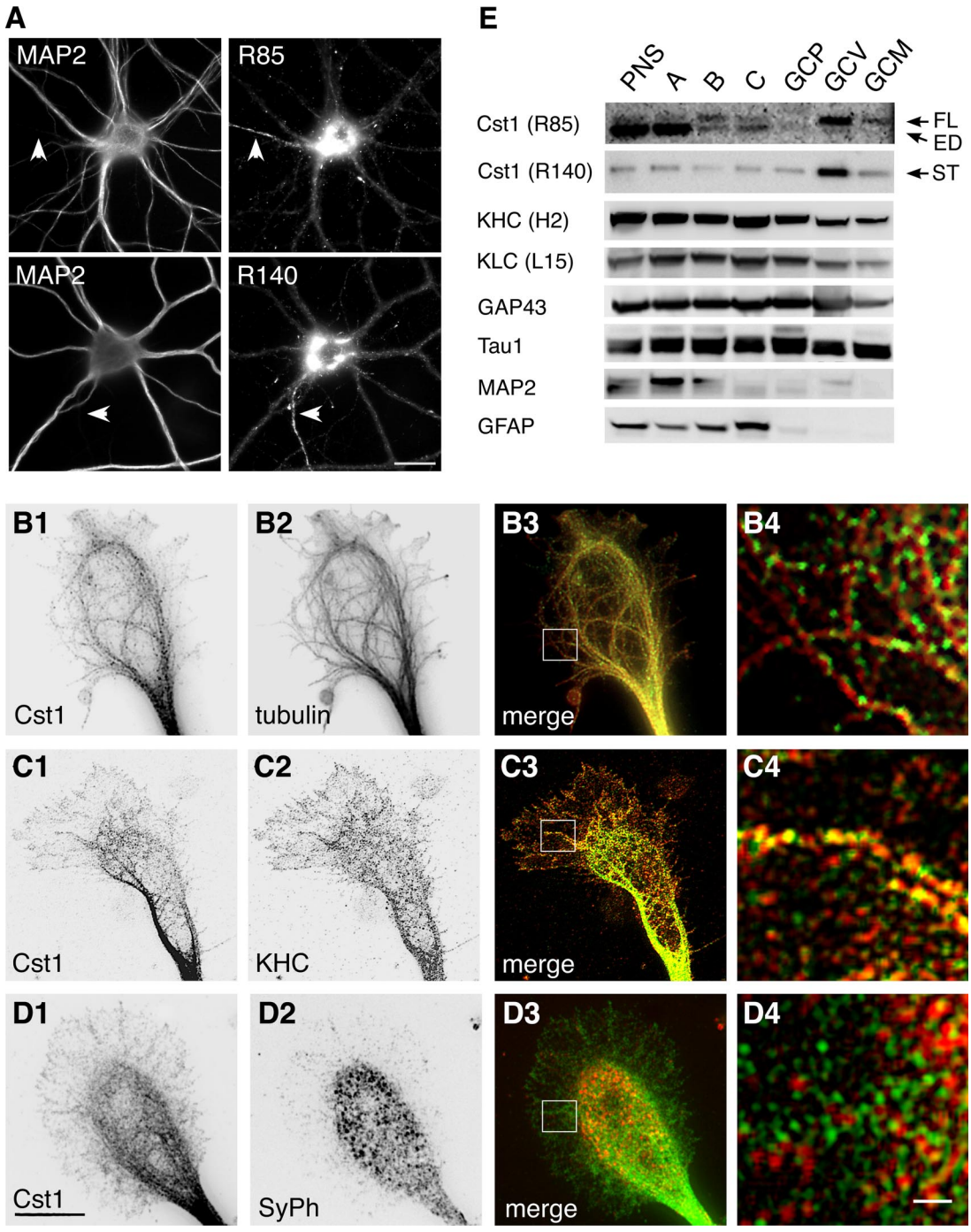

Figure 5. Calsyntenin-1 colocalizes with Kinesin-1 in growth cones and is enriched in axonal growth cone vesicles. (A) Immunocytochemistry of cultured cortical neurons (14 DIV) using antibodies R85 or R140. Dendrites and axons (arrowheads) were discriminated by costaining with MAP2. Anti-calsyntenin-1 antibodies labeled tubulovesicular structures in the soma, in dendrites, and in the axon. Note the abundance of calsyntenin-1 immunoreactivity in the perinuclear region and in the axon. Scale bar, 30 μm. (B–D) Double stainings of axonal growth cones (4 DIV) with antibody R85 (B1–D1) and either tubulin (B2), KHC (C2), or synaptophysin (SyPh; D2). Note the alignment of calsyntenin-1–positive vesicles along microtubules (B3 and B4) and the partial colocalization with KHC (C3 and C4), but not with synaptophysin (D3 and D4). B4 to D4 show higher magnifications of the boxed areas in B3 to D3. Scale bar, 10 μm in D1 and 1 μm in D4. (E) Axonal growth cones were isolated from P7 mouse brains by subcellular fractionation and analyzed by Western blotting using the indicated antibodies. Full-length (FL) calsyntenin-1 and the calsyntenin-1 stump (ST) were enriched in the GCV fraction, with trace amounts present in the GCM fraction. Note the presence of KLC and KHC in the GCV fraction. ED, ectodomain; PNS, postnuclear supernatant. (A) Growth cone particle-enriched fraction; (B) synaptic elements; (C) axonal shafts. GCP, pelleted growth cone particles; GCV, growth cone vesicles; GCM, growth cone membranes.

ity-purified antibody (R113) against the cytoplasmic part of calsyntenin-1 (Figure 4, A and B). In both developing and adult brain, calsyntenin-1 was highly expressed in the gray matter of all brain regions. However, a striking difference

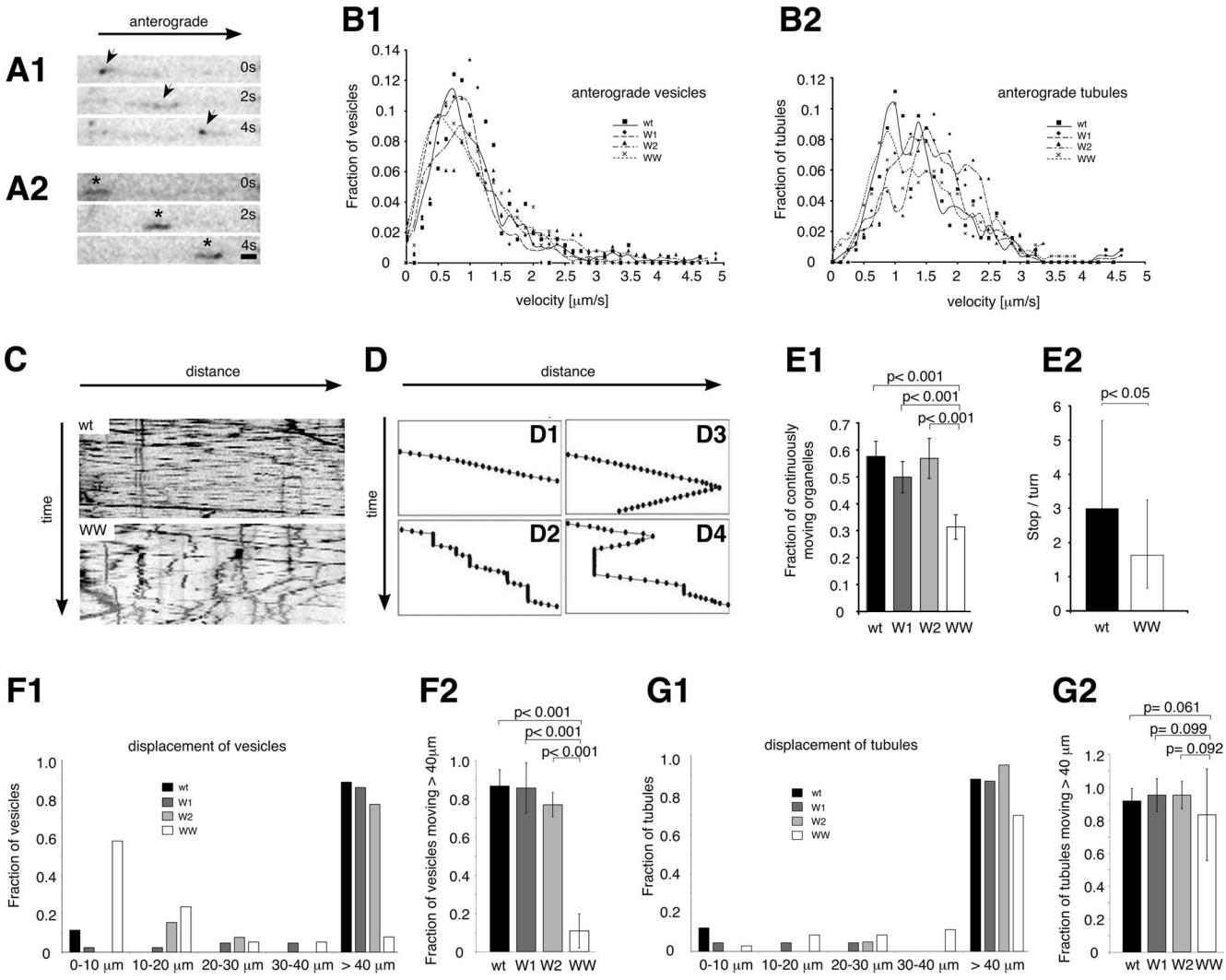

Figure 6. Axonal transport of calsyntenin-1–containing vesicles depends on the binding between the cytoplasmic segment of calsyntenin-1 and Kinesin-1. (A) Three consecutive frames of a time-lapse sequence (2-s interval) showing one moving vesicle (A1, arrowheads) and one tubular organelle (A2, ∗) containing EGFP-calsyntenin-1 moving anterogradely within the same axonal segment. (B) Velocity distribution of vesicles (B1) and tubules (B2) carrying wt, W1, W2, and WW EGFP-calsyntenin-1. (C) Kymographs illustrating the movements of wt (top) and WW (bottom) transport organelles. (D) Schematic representation of different types of trajectories obtained by manual organelle tracking (see *Materials and Methods*). (E) Quantitative analysis of organelle motility. (E1) At least 50% of wt, W1, and W2 transport organelles moved continuously, compared with 30% of WW organelles. WW organelles differed significantly from wt, W1, and W2 organelles (wt, n = 221; W1, n = 217; W2, n = 127; WW, n = 317). (E2) Ratio of stop-to-turn events for wt and WW mutant organelles. After pausing, WW organelles initiated retrograde movement significantly more often than wt organelles. (F1 and G1) Displacement-distribution (run-lengths) of wt, W1, W2, and WW vesicles (F1) and tubules (G1). (F2) The displacement of WW vesicles was significantly reduced compared with wt, W1, and W2 vesicles. (wt, n = 96; W1, n = 42; W2, n = 31; WW, n = 36). (G2) WW tubules were not significantly different from wt, W1, and W2 tubules (wt, n = 32; W1, n = 23; W2, n = 42; WW, n = 37). Error bars, SEM. Scale bar in A, 1 μm.

was found in the white matter. At P6, calsyntenin-1 was highly expressed in all major fiber tracts, including the anterior commissure and the corpus callosum, as well as the external and internal capsules (Figure 4A). In contrast, only faint axonal calsyntenin-1 immunoreactivity was detected in fiber tracts of adult mice (Figure 4B). We then analyzed the subcellular localization of calsyntenin-1 in corpus callosum by immunoelectron microscopy. At P8, the majority of nonmyelinated axonal profiles contained a large number of extensively labeled spherical and tubulovesicular organelles of a diameter of 0.065 ± 0.016 μm (mean ± SD, n = 64, range 0.035–0.122 μm) and a length of 0.195 ± 0.070 μm (mean ± SD, n = 64, range 0.079–0.331 μm; Figure 4, C and E). In the adult brain, immunogold-labeled organelles had a similar ultrastructural appearance and size (Figure 4, D and F). However, the number of these organelles per axonal profile was very low, consistent with the observed weak immunoreactivity in the white matter of adult brain at the light microscopic level. In conclusion, our immuno-localization studies demonstrate the association of calsyntenin-1 with tubulovesicular organelles in vivo, particularly in developing axons.

Calsyntenin-1 Is Enriched in Axonal Growth Cone Vesicles

The presence of calsyntenin-1–containing organelles in developing axons led us to presume that these organelles are

targeted to the growing tips, the growth cones. To test this, we performed immunocytochemistry of cultured primary neurons using antibodies R85 and R140 (Figure 5A). Both antibodies produced a vesicular staining pattern and a strong immunoreactivity in the perinuclear region, most likely in the Golgi apparatus. Tubulovesicular structures were labeled in cell bodies, in dendrites, and in axons, where calsyntenin-1 immunoreactivity was clearly enriched. In axonal growth cones, calsyntenin-1–positive vesicles were aligned along microtubules, particularly in the central region (Figure 5, B1–B4). Calsyntenin-1 partially colocalized with KHC in the same vesicles (Figure 5, C1–C4) but did not colocalize with synaptophysin (Figure 5, D1–D4). We next isolated growth cone vesicles from P7 mouse forebrains (Igarashi *et al.*, 1997). The integrity and the quality of the GCPs and GCVs was confirmed by electron microscopy (unpublished data) and by Western blotting as described previously (Pfenninger *et al.*, 1983; Lohse *et al.*, 1996; Igarashi *et al.*, 1997). As shown in Figure 5E, the full-length form and the transmembrane stump of calsyntenin-1 were highly enriched in the GCV fraction, which also contained a substantial amount of KLC and KHC. Altogether, these results indicate that calsyntenin-1–containing organelles constitute a pool of axonal growth cone vesicles that are distinct from synaptic vesicle precursors.

The Transport of Calsyntenin-1 Vesicles Critically Depends on the Binding between the Cytoplasmic Domain of Calsyntenin-1 and Kinesin-1

Based on the reduced KLC1-binding of the calsyntenin-1 WW mutant (Figure 2, D–F), we presumed that organelles bearing this form of calsyntenin-1 would be transported less efficiently. To test this, we transfected primary cortical neurons with EGFP-tagged wt or mutant calsyntenin-1 (W1, W2, and WW) and analyzed vesicular transport along the axons by time-lapse microscopy. Ectopically expressed EGFP-calsyntenin-1 fusion proteins displayed a cellular distribution similar to endogenous calsyntenin-1. EGFP-labeled transport organelles varied in size and shape, from elongated tubules to round vesicles (Figure 6, A1 and A2). Vesicular and tubular organelles were moving along the axon mostly anterogradely, but occasionally switched to the retrograde direction. Figure 6A shows three consecutive frames from a time-lapse recording of a vesicle (A1) and a tubule (A2) moving in anterograde direction within the same axon of an EGFP-calsyntenin-1–transfected neuron.

We determined the velocities of vesicles and tubules carrying wt, single-mutated (W1 and W2) and double-mutated (WW) EGFP-calsyntenin-1 (Figure 6, B1 and B2; Table 1). Anterograde velocities ranged from 0.96 ± 0.6 to 1.27 ± 0.86 μm/s for vesicles and from 1.43 ± 0.79 to 1.66 ± 0.64 μm/s for tubules, consistent with the speed reported for fast anterograde axonal transport (Grafstein and Forman, 1980; Allen *et al.*, 1982; Nakata *et al.*, 1998; Kaether *et al.*, 2000). Neither anterograde nor retrograde velocities differed significantly between wt and mutant organelles. Interestingly, however, kymographs revealed a different pattern of movement of wt versus WW organelles. Organelles bearing wt (Figure 6, C, top, and D1; Supplementary Movie 1), W1, and W2 mutants (unpublished data) preferably moved along axons in a straight trajectory with relatively few stops. In contrast, WW organelles made several stops along their trajectory (Figure 6, C, bottom, and D2–D4; Supplementary Movie 2). After pausing for a variable time, a fraction of these organelles resumed migration in the same direction (Figure 6D2), whereas others moved in the opposite direction (Figure 6, D3 and D4). A third group of WW organelles

Table 1. Characteristics of wild-type and mutant EGFP-calsyntenin-1–containing vesicles and tubules in cultured primary neurons

Construct:	wt		W1		W2		WW	
Organelle:	Vesicles	Tubules	Vesicles	Tubules	Vesicles	Tubules	Vesicles	Tubules
Velocity (μm/s)								
ag	1.12 ± 0.71 (256)	1.43 ± 0.79 (162)	0.96 ± 0.6 (165)	1.57 ± 0.71 (241)	1.27 ± 0.86 (378)	1.66 ± 0.64 (166)	1.02 ± 0.65 (464)	1.44 ± 0.75 (312)
rg	0.72 ± 0.51 (74)		0.82 ± 0.48 (129)		0.71 ± 0.50 (86)		0.64 ± 0.46 (141)	
Displacement (μm)								
ag	56.9 ± 26.83 (96)	59.91 ± 21.73 (54)	52.06 ± 15.98 (51)	55.52 ± 11.77 (44)	45.03 ± 15.45 (41)	44.54 ± 8.75 (42)	13.11 ± 12.67 (48)	39.55 ± 12.68 (56)

Number of organelles in parentheses. wt, wild type; W1, W2, WW, mutant; ag, anterograde; rg, retrograde.

remained at rest after a stop for the entire period of observation. For a quantitative assessment, we categorized the patterns of organelle movements into two groups. One group comprised organelles that moved continuously during the period of image acquisition. The other group comprised organelles that stopped at least once, including those that resumed migration and those that remained immobile. In the time frame of 3 min, 50–60% of wt, W1 and W2 organelles moved without a stop. In contrast, only 30% of WW organelles moved continuously (Figure 6E1). In addition, resting WW organelles more often switched to retrograde movement than wt organelles (Figure 6E2).

We then analyzed in detail the individual run-lengths of calsyntenin-1 vesicles and tubules by measuring the distance traveled before stopping or turning (Figure 6, F and G; Table 1). The length of the observed axonal segments varied from 40 to 116 μm. Therefore, we arbitrarily set 40 μm as maximum displacement and pooled all organelles moving 40 μm or more. We found that more than 75% of wt, W1, and W2 vesicles, but only 11% of WW vesicles, moved more than 40 μm without stopping (Figure 6F1). Strikingly, 57% of WW vesicles moved only 10 μm or less without a stop. We then quantitatively analyzed vesicles that moved more than 40 μm from five individual experiments. The run-lengths of WW vesicles were significantly reduced compared with wt vesicles ($p < 0.001$), whereas no difference was found between wt, W1, and W2 vesicles (Figure 6F2). Interestingly, the same analysis performed on tubular organelles revealed no significant difference between the four calsyntenin-1 constructs (Figure 6, G1 and G2). Taken together, these data indicate that interference with the motor binding function of calsyntenin-1 disrupts processive transport of a subset of axonal vesicles.

DISCUSSION

Calsyntenin-1 Interacts with the Kinesin-1 Motor through Binding to KLC1

Using a combination of yeast two-hybrid screen, GST pull-downs and immunoprecipitation experiments, we demonstrated a specific interaction between calsyntenin-1 and the TPR domains of KLC1. In the cytoplasmic segment of calsyntenin-1, we identified two kinesin-binding segments (KBS1 and KBS2) that consist of the short peptide sequences KENEMDWDDS and ATRQLEWDDS, respectively. Sequence comparison of the cytoplasmic parts of calsyntenin orthologues revealed a strong conservation of both kinesin-binding segments (Figure 2) that can be defined by the consensus sequence L/M–E/D–W–D–D–S (Figure 7). We showed that amino acid positions M901, W903, D904, and D905 in calsyntenin-1 are crucial for the interaction with KLC1, whereas E900 and D902 appeared less important. Interestingly, position 2 (D902) is the least conserved position in KBS1. Apart from an acidic residue preserved in mammalian calsyntenin-1 and -2, isoleucine and histidine is found in *Drosophila melanogaster* and *Caenorhabditis elegans*, respectively. At this position, calsyntenin-3 contains a phenylalanine (F896), which is responsible, at least in part, for the lower apparent binding affinity of calsyntenin-3 to KLC1. In KBS2, the only deviation from the consensus sequence is found at position 5 in *D. melanogaster* and at position 6 in *C. elegans*. Based on this high degree of conservation of the KLC1-binding sites during evolution and the observations that one functional KBS is sufficient to mediate binding of a calsyntenin molecule to KLC1, it is likely that all members of the calsyntenin family interact with Kinesin-1.

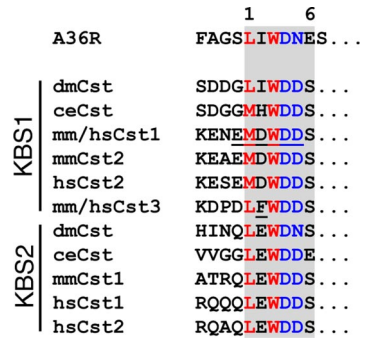

Figure 7. KBS1 and KBS2 are conserved among calsyntenins and show sequence similarity to the vaccinia virus protein A36R. Alignment of KBS1 and KBS2 core motives of all calsyntenin members with an internal sequence (aa 95-101) of the vaccinia virus protein A36R. Note the sequence similarity at positions 1, 3, 4, and 5 in KLC-binding motives between calsyntenins and A36R. Underlined amino acid residues highlight important positions for the interaction.

The binding motives recognized by KLC1 in the cytoplasmic segment of the calsyntenins may also be used for the docking of other cargo. We found an intriguing sequence similarity of the calsyntenin KBS to at least one other ligand of the TPRs of KLC1 (Figure 7), the vaccinia virus envelope protein A36R (Ward and Moss, 2004). Because the KLC-binding site of A36R has not been mapped in detail, we aligned the minimal amino acid segment reported to bind KLC1 (aa 81-110) with the KBS consensus sequence. We recognized a LIWDNES motif (aa 95-101), which is very similar to the calsyntenin KBS. Leucine (position 1), tryptophan (position 3), and aspartate (position 4) match the KBS consensus. Isoleucine (position 2) is in accordance with the KBS1 of *D. melanogaster* calsyntenin. Asparagine at position 5 is in accordance with the corresponding amino acid in the KBS2 of *D. melanogaster*, and glutamate at position 6 has its counterpart in KBS2 of *C. elegans*. In contrast, the KLC1 binding motif of JIP-1/-2, which is also well preserved among the JIP family members (Verhey *et al.*, 2001), is distinct from the one found in calsyntenins and in A36R. It is noteworthy that calsyntenins and A36R bind to KLC via highly similar internal sequences, whereas the KLC1-binding motif of JIP-1/-2 is located at the very C-terminus. At present, it is unknown how TPRs of KLC1 bind to these structurally unrelated ligands. The high degree of sequence conservation among the JIP-1/-2- and the calsyntenin-types of KLC-binding motives implies that they both have been subject to strong evolutionary constraint in order to maintain the functional interaction with KLC1. The preservation of two KLC1 binding motives in calsyntenin-1 is intriguing and suggests a distinct mechanism of complex formation.

A quantitative analysis of the interaction between the isolated cytoplasmic segment of calsyntenin-1 and KLC1 indicated a relatively weak affinity, as reflected by a dissociation constant of ~1.7 μM. However, a vesicular docking contact with a Kinesin-1 motor may involve multiple calsyntenin-1 molecules, as we found saturation of KLC1 to calsyntenin-1 binding at a molar ratio of 0.5. This indicates that each KLC1 binds the cytoplasmic segments of two calsyntenins. Based on the crystal structure of the three TPRs of protein phosphatase-5, it has been suggested that tandemly arranged TPR motifs are organized into a regular right-handed superhelix that could accommodate multiple ligands (Das *et al.*, 1998). Thus, it is conceivable that the six TPR repeats of one KLC1 molecule can indeed bind the

cytoplasmic segments of two calsyntenin-1 molecules simultaneously. Because a Kinesin-1 motor contains two light chains, our results suggest a model for a vesicular docking complex in which four calsyntenins are attached to one Kinesin-1 motor. Such an arrangement of calsyntenin in the membrane may be stabilized by lateral homophilic interactions between the cadherin domains of neighboring calsyntenin molecules (Patel *et al.*, 2003). The multiplicity of the calsyntenin-1–mediated docking contacts thereby could compensate for the relatively low affinity measured for the individual contacts in vitro.

Calsyntenin-1 Associates with Tubulovesicular Organelles In Vivo

We previously localized the calsyntenins to postsynaptic membranes in the adult mouse brain (Vogt *et al.*, 2001; Hintsch *et al.*, 2002). Here we demonstrate that in young brains, calsyntenin-1 is enriched in axonal fiber tracts. This may indicate a redistribution of calsyntenin-1 from axonal to dendritic compartments during development. Further experiments will be required for confirmation of this idea.

Our developmental analyses revealed that the spatiotemporal expression patterns of calsyntenin-1 and Kinesin-1 are congruent (Vignali *et al.*, 1997; Kanai *et al.*, 2000; Morfini *et al.*, 2001a). Colocalization with KHC, as well as the presence of both KLC and KHC on GCV membranes, support the idea that calsyntenin-1–containing vesicles are transported to axonal growth cones by Kinesin-1. At the ultrastructural level, calsyntenin-1 was associated with tubulovesicular organelles. Their size and appearance correspond to anterogradely transported membrane structures described in earlier electron-microscopic analyses (Tsukita and Ishikawa, 1980; Lindsey and Ellisman, 1985; Miller and Lasek, 1985). These organelles were shown to be morphologically distinct from endosomal compartments and retrogradely moving, large multivesicular bodies. Tubular organelles have been previously described as transport carriers for synaptophysin (Nakata *et al.*, 1998; Kaether *et al.*, 2000). We did not detect any significant colocalization of calsyntenin-1 with synaptophysin in cultured neurons (Figure 5; our unpublished data), suggesting that calsyntenin-1–positive organelles are different from synaptic vesicle precursors. It will be of interest to identify the type of cargo that is transported by calsyntenin-1.

Calsyntenin-1 Mediates Processive Transport of Tubulovesicular Organelles

Anterograde velocities and run-lengths of organelles recorded in live cells (Nakata *et al.*, 1998; Kaether *et al.*, 2000; Hill *et al.*, 2004; Kural *et al.*, 2005) are often higher than those determined for single motors in vitro (Howard *et al.*, 1989; Block *et al.*, 1990). It has been proposed that this is due to the cooperative action of several motor proteins working in vivo. This view is supported by electron-microscopic studies showing that cargo can be linked to microtubules by several cross-bridges (Miller and Lasek, 1985; Ashkin *et al.*, 1990) and by the observation that kinesin density determines the velocity of transport in vitro (Hunt *et al.*, 1994) and in vivo (Kural *et al.*, 2005). Theoretical studies further suggest that motor cooperativity strongly increases cargo run-lengths (Lipowsky *et al.*, 2001; Klumpp and Lipowsky, 2005). In addition, motor number appears to correlate with cargo size, because larger organelles, such as tubules, have repeatedly been observed to move with slightly faster average velocities than vesicles (Kaether *et al.*, 2000; Kreitzer *et al.*, 2000). Therefore, the number of motor-cargo connections appears to define both the velocity and the run-length of the cargo.

We found that ~90% of the vesicles with WW-mutant calsyntenin-1 moved with significantly reduced anterograde run-lengths compared with wt and single mutant vesicles. Because overexpression of the WW mutant produces a vast excess of exogenous over endogenous protein, vesicular transport under this condition may largely depend on the WW mutant, which is severely impaired in KLC1 binding. In view of our aforementioned model of the calsyntenin-1–dependent vesicular docking complex, dilution of endogenous calsyntenin-1 by WW-mutated calsyntenin-1 is likely to weaken the contacts between the vesicular calsyntenin-1–docking quadruplet and the individual Kinesin-1 motor. As a consequence, there is an increased probability for dissociation of individual cargo-motor complexes, which results in a decrease in motor cooperativity and thus puts vesicles with WW-mutant calsyntenin-1 at higher risk to dissociate from the microtubule track. This model is compatible with our observation that run-lengths of tubules were not significantly affected by overexpression of the WW mutant. Tubules may be less sensitive to dissociation than vesicles because of their larger surface and, therefore, the larger number of associated Kinesin-1 motors. In other words, the loss of individual motors from tubules may be tolerated because of the compensatory function of residual motor contacts. Thus, the abundance of motor-cargo connections on tubules may be regarded as a safety factor protecting them against dissociation from the microtubule.

An alternative interpretation of our data might be that the mutated calsyntenins are missorted into another type of vesicle that exhibits a different migratory pattern. We consider missorting unlikely because of the following reasons: 1) Wild-type and WW mutant proteins displayed a very similar cellular distribution when transfected into neurons. Both proteins were found in the axon, where they were associated with tubulovesicular organelles that moved with almost identical average velocities. 2) In transfected cell lines, such as HeLa, wt and WW mutant proteins localize to the ER and the Golgi and are transported to the plasma membrane. 3) Both proteins are subject to proteolytic processing, as the stump and the cleaved ectodomain can be detected in cell lysates and cell supernatants, respectively (our unpublished data). These data suggest that the WW mutation does not notably alter sorting of calsyntenin-1.

Recent findings indicate that motors with opposite polarity are coordinated (Gross *et al.*, 2002; Welte, 2004; Kural *et al.*, 2005; Miller *et al.*, 2005) and that they reside on the same organelles (Hirokawa *et al.*, 1990; Muresan *et al.*, 1996). In addition, there are intriguing hints for their physical interactions (Deacon *et al.*, 2003; Ligon *et al.*, 2004). However, the molecular mechanisms for the reciprocal regulation of their activities are unclear. We found that WW vesicles were significantly more likely to resume movement in retrograde direction after a stop than wt vesicles. This suggests that perturbation of the calsyntenin-1/Kinesin-1 interaction induces a switch in motor usage in favor of dynein. This is in line with a previous report demonstrating that loss of the cargo-docking protein liprin alpha in *C. elegans* results in decreased anterograde processivity and an increase in retrograde transport initiation of synaptic vesicle precursors (Shin *et al.*, 2003; Miller *et al.*, 2005). Taken together, these data suggest that interference with the function of a cargo-docking molecule for an anterograde motor may not only disrupt processive transport in this direction but also facilitate the reversal of direction.

In conclusion, our data define calsyntenin-1 as a novel cargo-docking protein for processive, Kinesin-1–mediated transport of vesicles and tubulovesicular organelles. Calsyn-

tenin-1–containing organelles may support axonal growth and guidance by translocating vesicular cargo destined for the growth cone.

ACKNOWLEDGMENTS

We thank S. T. Brady for the KLC 63-90 antibody and valuable technical suggestions, B. J. Schnapp for providing the HA-L176 and myc-KHC constructs, and A. Baici for helpful comments. This research was supported by the Swiss National Science Foundation, the NCCR Neural Plasticity and Repair, and the Transregio-Sonderforschungsbereich Konstanz-Zürich (TR SFB 11).

REFERENCES

Allen, R. D., Metuzals, J., Tasaki, I., Brady, S. T., and Gilbert, S. P. (1982). Fast axonal transport in squid giant axon. Science *218*, 1127–1129.

Araki, Y., Tomita, S., Yamaguchi, H., Miyagi, N., Sumioka, A., Kirino, Y., and Suzuki, T. (2003). Novel cadherin-related membrane proteins, Alcadeins, enhance the X11-like protein-mediated stabilization of amyloid beta-protein precursor metabolism. J. Biol. Chem. *278*, 49448–49458.

Ashkin, A., Schutze, K., Dziedzic, J. M., Euteneuer, U., and Schliwa, M. (1990). Force generation of organelle transport measured in vivo by an infrared laser trap. Nature *348*, 346–348.

Banker, G. A. (1980). Trophic interactions between astroglial cells and hippocampal neurons in culture. Science *209*, 809–810.

Blatch, G. L., and Lassle, M. (1999). The tetratricopeptide repeat: a structural motif mediating protein-protein interactions. Bioessays *21*, 932–939.

Block, S. M., Goldstein, L. S., and Schnapp, B. J. (1990). Bead movement by single kinesin molecules studied with optical tweezers. Nature *348*, 348–352.

Bowman, A. B., Kamal, A., Ritchings, B. W., Philp, A. V., McGrail, M., Gindhart, J. G., and Goldstein, L. S. (2000). Kinesin-dependent axonal transport is mediated by the sunday driver (SYD) protein. Cell *103*, 583–594.

Bradke, F., and Dotti, C. G. (2000). Establishment of neuronal polarity: lessons from cultured hippocampal neurons. Curr. Opin. Neurobiol. *10*, 574–581.

Brady, S. T. (1985). A novel brain ATPase with properties expected for the fast axonal transport motor. Nature *317*, 73–75.

Das, A. K., Cohen, P. W., and Barford, D. (1998). The structure of the tetratricopeptide repeats of protein phosphatase 5, implications for TPR-mediated protein-protein interactions. EMBO J. *17*, 1192–1199.

Deacon, S. W., Serpinskaya, A. S., Vaughan, P. S., Lopez Fanarraga, M., Vernos, I., Vaughan, K. T., and Gelfand, V. I. (2003). Dynactin is required for bidirectional organelle transport. J. Cell Biol. *160*, 297–301.

Diefenbach, R. J., Diefenbach, E., Douglas, M. W., and Cunningham, A. L. (2002). The heavy chain of conventional kinesin interacts with the SNARE proteins SNAP25 and SNAP23. Biochemistry *41*, 14906–14915.

Grafstein, B., and Forman, D. S. (1980). Intracellular transport in neurons. Physiol. Rev. *60*, 1167–1283.

Gross, S. P., Welte, M. A., Block, S. M., and Wieschaus, E. F. (2002). Coordination of opposite-polarity microtubule motors. J. Cell Biol. *156*, 715–724.

Hill, D. B., Plaza, M. J., Bonin, K., and Holzwarth, G. (2004). Fast vesicle transport in PC12 neurites: velocities and forces. Eur. Biophys. J. *33*, 623–632.

Hintsch, G., Zurlinden, A., Meskenaite, V., Steuble, M., Fink-Widmer, K., Kinter, J., and Sonderegger, P. (2002). The calsyntenins—a family of postsynaptic membrane proteins with distinct neuronal expression patterns. Mol. Cell Neurosci. *21*, 393–409.

Hirokawa, N. (1998). Kinesin and dynein superfamily proteins and the mechanism of organelle transport. Science *279*, 519–526.

Hirokawa, N., Pfister, K. K., Yorifuji, H., Wagner, M. C., Brady, S. T., and Bloom, G. S. (1989). Submolecular domains of bovine brain kinesin identified by electron microscopy and mAb decoration. Cell *56*, 867–878.

Hirokawa, N., Sato-Yoshitake, R., Yoshida, T., and Kawashima, T. (1990). Brain dynein (MAP1C) localizes on both anterogradely and retrogradely transported membranous organelles in vivo. J. Cell Biol. *111*, 1027–1037.

Hirokawa, N., and Takemura, R. (2005). Molecular motors and mechanisms of directional transport in neurons. Nat. Rev. Neurosci. *6*, 201–214.

Howard, J., Hudspeth, A. J., and Vale, R. D. (1989). Movement of microtubules by single kinesin molecules. Nature *342*, 154–158.

Hunt, A. J., Gittes, F., and Howard, J. (1994). The force exerted by a single kinesin molecule against a viscous load. Biophys. J. *67*, 766–781.

Igarashi, M., Tagaya, M., and Komiya, Y. (1997). The soluble N-ethylmaleimide-sensitive factor attached protein receptor complex in growth cones: molecular aspects of the axon terminal development. J. Neurosci. *17*, 1460–1470.

Inomata, H., Nakamura, Y., Hayakawa, A., Takata, H., Suzuki, T., Miyazawa, K., and Kitamura, N. (2003). A scaffold protein JIP-1b enhances amyloid precursor protein phosphorylation by JNK and its association with kinesin light chain 1. J. Biol. Chem. *278*, 22946–22955.

Jan, Y. N., and Jan, L. Y. (2001). Dendrites. Genes Dev. *15*, 2627–2641.

Kaether, C., Skehel, P., and Dotti, C. G. (2000). Axonal membrane proteins are transported in distinct carriers: a two-color video microscopy study in cultured hippocampal neurons. Mol. Biol. Cell *11*, 1213–1224.

Kamal, A., Almenar-Queralt, A., LeBlanc, J. F., Roberts, E. A., and Goldstein, L. S. (2001). Kinesin-mediated axonal transport of a membrane compartment containing beta-secretase and presenilin-1 requires APP. Nature *414*, 643–648.

Kamal, A., Stokin, G. B., Yang, Z., Xia, C. H., and Goldstein, L. S. (2000). Axonal transport of amyloid precursor protein is mediated by direct binding to the kinesin light chain subunit of kinesin-I. Neuron *28*, 449–459.

Kanai, Y., Okada, Y., Tanaka, Y., Harada, A., Terada, S., and Hirokawa, N. (2000). KIF5C, a novel neuronal kinesin enriched in motor neurons. J. Neurosci. *20*, 6374–6384.

Klumpp, S., and Lipowsky, R. (2005). Cooperative cargo transport by several molecular motors. Proc. Natl. Acad. Sci. USA *102*, 17284–17289.

Kreitzer, G., Marmorstein, A., Okamoto, P., Vallee, R., and Rodriguez-Boulan, E. (2000). Kinesin and dynamin are required for post-Golgi transport of a plasma-membrane protein. Nat. Cell Biol. *2*, 125–127.

Kural, C., Kim, H., Syed, S., Goshima, G., Gelfand, V. I., and Selvin, P. R. (2005). Kinesin and dynein move a peroxisome in vivo: a tug-of-war or coordinated movement? Science *308*, 1469–1472.

Lazarov, O. *et al.* (2005). Axonal transport, amyloid precursor protein, kinesin-1, and the processing apparatus: revisited. J. Neurosci. *25*, 2386–2395.

Ligon, L. A., Tokito, M., Finklestein, J. M., Grossman, F. E., and Holzbaur, E. L. (2004). A direct interaction between cytoplasmic dynein and kinesin I may coordinate motor activity. J. Biol. Chem. *279*, 19201–19208.

Lindsey, J. D., and Ellisman, M. H. (1985). The neuronal endomembrane system. I. Direct links between rough endoplasmic reticulum and the cis element of the Golgi apparatus. J. Neurosci. *5*, 3111–3123.

Lipowsky, R., Klumpp, S., and Nieuwenhuizen, T. M. (2001). Random walks of cytoskeletal motors in open and closed compartments. Phys. Rev. Lett. *87*, 108101.

Lohse, K., Helmke, S. M., Wood, M. R., Quiroga, S., de la Houssaye, B. A., Miller, V. E., Negre-Aminou, P., and Pfenninger, K. H. (1996). Axonal origin and purity of growth cones isolated from fetal rat brain. Brain Res. Dev. Brain Res. *96*, 83–96.

Martinez-Arca, S., *et al.* (2001). A common exocytotic mechanism mediates axonal and dendritic outgrowth. J. Neurosci. *21*, 3830–3838.

Matsuda, S., Matsuda, Y., and D'Adamio, L. (2003). Amyloid beta protein precursor (AbetaPP), but not AbetaPP-like protein 2, is bridged to the kinesin light chain by the scaffold protein JNK-interacting protein 1. J. Biol. Chem. *278*, 38601–38606.

Miller, K. E., DeProto, J., Kaufmann, N., Patel, B. N., Duckworth, A., and Van Vactor, D. (2005). Direct observation demonstrates that Liprin-alpha is required for trafficking of synaptic vesicles. Curr. Biol. *15*, 684–689.

Miller, R. H., and Lasek, R. J. (1985). Cross-bridges mediate anterograde and retrograde vesicle transport along microtubules in squid axoplasm. J. Cell Biol. *101*, 2181–2193.

Morfini, G., Szebenyi, G., Richards, B., and Brady, S. T. (2001a). Regulation of kinesin: implications for neuronal development. Dev. Neurosci. *23*, 364–376.

Morfini, G., Tsai, M. Y., Szebenyi, G., and Brady, S. T. (2001b). Approaches to study interactions between kinesin motors and membranes. Methods Mol. Biol. *164*, 147–162.

Muresan, V., Godek, C. P., Reese, T. S., and Schnapp, B. J. (1996). Plus-end motors override minus-end motors during transport of squid axon vesicles on microtubules. J. Cell Biol. *135*, 383–397.

Nakata, T., Terada, S., and Hirokawa, N. (1998). Visualization of the dynamics of synaptic vesicle and plasma membrane proteins in living axons. J. Cell Biol. *140*, 659–674.

Patel, S. D., Chen, C. P., Bahna, F., Honig, B., and Shapiro, L. (2003). Cadherin-mediated cell-cell adhesion: sticking together as a family. Curr. Opin. Struct. Biol. *13*, 690–698.

Pfenninger, K. H., Ellis, L., Johnson, M. P., Friedman, L. B., and Somlo, S. (1983). Nerve growth cones isolated from fetal rat brain: subcellular fractionation and characterization. Cell *35*, 573–584.

Rahman, A., Friedman, D. S., and Goldstein, L. S. (1998). Two kinesin light chain genes in mice. Identification and characterization of the encoded proteins. J. Biol. Chem. *273*, 15395–15403.

Scheufler, C., Brinker, A., Bourenkov, G., Pegoraro, S., Moroder, L., Bartunik, H., Hartl, F. U., and Moarefi, I. (2000). Structure of TPR domain-peptide complexes: critical elements in the assembly of the Hsp70-Hsp90 multichaperone machine. Cell *101*, 199–210.

Scott, E. K., and Luo, L. (2001). How do dendrites take their shape? Nat. Neurosci. *4*, 359–365.

Setou, M., Seog, D. H., Tanaka, Y., Kanai, Y., Takei, Y., Kawagishi, M., and Hirokawa, N. (2002). Glutamate-receptor-interacting protein GRIP1 directly steers kinesin to dendrites. Nature *417*, 83–87.

Shin, H., *et al.* (2003). Association of the kinesin motor KIF1A with the multimodular protein liprin-alpha. J. Biol. Chem. *278*, 11393–11401.

Stockinger, W., Brandes, C., Fasching, D., Hermann, M., Gotthardt, M., Herz, J., Schneider, W. J., and Nimpf, J. (2000). The reelin receptor ApoER2 recruits JNK-interacting proteins-1 and -2. J. Biol. Chem. *275*, 25625–25632.

Terlecky, S. R., Nuttley, W. M., McCollum, D., Sock, E., and Subramani, S. (1995). The *Pichia pastoris* peroxisomal protein PAS8p is the receptor for the C-terminal tripeptide peroxisomal targeting signal. EMBO J. *14*, 3627–3634.

Tsai, M. Y., Morfini, G., Szebenyi, G., and Brady, S. T. (2000). Release of kinesin from vesicles by hsc70 and regulation of fast axonal transport. Mol. Biol. Cell *11*, 2161–2173.

Tsukita, S., and Ishikawa, H. (1980). The movement of membranous organelles in axons. Electron microscopic identification of anterogradely and retrogradely transported organelles. J. Cell Biol. *84*, 513–530.

Vale, R. D., Reese, T. S., and Sheetz, M. P. (1985). Identification of a novel force-generating protein, kinesin, involved in microtubule-based motility. Cell *42*, 39–50.

Verhey, K. J., Lizotte, D. L., Abramson, T., Barenboim, L., Schnapp, B. J., and Rapoport, T. A. (1998). Light chain-dependent regulation of Kinesin's interaction with microtubules. J. Cell Biol. *143*, 1053–1066.

Verhey, K. J., Meyer, D., Deehan, R., Blenis, J., Schnapp, B. J., Rapoport, T. A., and Margolis, B. (2001). Cargo of kinesin identified as JIP scaffolding proteins and associated signaling molecules. J. Cell Biol. *152*, 959–970.

Vignali, G., Lizier, C., Sprocati, M. T., Sirtori, C., Battaglia, G., and Navone, F. (1997). Expression of neuronal kinesin heavy chain is developmentally regulated in the central nervous system of the rat. J. Neurochem. *69*, 1840–1849.

Vogt, L., *et al.* (1996). Continuous renewal of the axonal pathway sensor apparatus by insertion of new sensor molecules into the growth cone membrane. Curr. Biol. *6*, 1153–1158.

Vogt, L., Schrimpf, S. P., Meskenaite, V., Frischknecht, R., Kinter, J., Leone, D. P., Ziegler, U., and Sonderegger, P. (2001). Calsyntenin-1, a proteolytically processed postsynaptic membrane protein with a cytoplasmic calcium-binding domain. Mol. Cell Neurosci. *17*, 151–166.

Ward, B. M., and Moss, B. (2004). Vaccinia virus A36R membrane protein provides a direct link between intracellular enveloped virions and the microtubule motor kinesin. J. Virol. *78*, 2486–2493.

Welte, M. A. (2004). Bidirectional transport along microtubules. Curr. Biol. *14*, R525–537.

Xia, C., Rahman, A., Yang, Z., and Goldstein, L. S. (1998). Chromosomal localization reveals three kinesin heavy chain genes in mouse. Genomics *52*, 209–213.